Bifurcation Analysis and Hormetic Effects in a Discrete-time Plant Quality and Larch Budmoth Interaction Model

Xiaohua Ren, Changcheng Xiang*, Yi Yang*

Abstract—**In recent years, the control of the larch budmoth has attracted a great deal of attention from experts, and spraying with insecticides is one of the main control strategies. The key of this strategy is the timing and efficiency of insecticide applications and how multiple insecticide applications affect the growth of budmoth. This paper extends a new two-dimensional discrete model by adding chemical controls based on a dynamical model of plant quality interacting with larch budmoth proposed in the literature to cope with this problem. First, the parametric conditions required for the existence and local stability of the positive fixed point of the model are discussed, and under certain conditions, the presence of period-doubling bifurcation and Neimark-Sacker bifurcation of the system, which reveals a significant effect of the kill rates of insecticides on the budmoth growth. The results show that a paradox arises when low kill rates stimulate the growth of budmoth and high kill rates inhibit the growth of budmoth. Furthermore, we analyze the influence of various factors and cumulative effects on the paradox phenomenon. Therefore, the timing of insecticide application and its efficiency should be chosen wisely to prevent the paradox.**

Index Terms—**discrete-time models; fixed points; local asymptotic stability; cumulative effects; Neimark-Sacker bifurcation; period-doubling bifurcation.**

I. Introduction

THE problem of pest outbreaks remains a popular research topic and it is essential in disciplines such as fisheries, agriculture and ecology [1]. Many agricultural experts have conducted studies on pest management [2]–[6] to address the damage to our ecosystem and the reduction in biodiversity owing to the various pests that attack fields and crops every year. It is well known that agricultural control, physical control, biological control and chemical control are the four main pest control strategies. In traditional pest management, spraying of insecticides is a widely used chemical control strategy. However, it can result in an increase in the pests' resistance or decrease in the number of the pests' natural enemies. Such irregularities may put populations at a high-risk of extinction, particularly in the context of examining the reproduction of organisms [7]–[9]. Therefore, the improper use of pesticides can lead to an increase in pests [10], [11]. This unexpected phenomenon is called pest resurgence [12]. Hormesis is an important cause of this phenomenon [13], [14].

Many previous studies have investigated the relationship between the larch budmoth and plant quality [15]–[17]. By contrast, our study focuses on the effects of insecticide mortality and the different timings and cumulative effects of insecticide application on the larch budmoth and plant quality. For the larch budmoth, i.e., a population with non-overlapping epochs, discrete-time difference equation models are more compatible than continuous-time difference equation models [18]–[20]. Discrete dynamical systems can represent intricate dynamical behaviors, such as chaos, Hopf bifurcation, flip bifurcation, and transcritical bifurcation, more graphically and vividly [21], [22].

It is well known that mathematical models can be used to better study the impacts of both the effectiveness of insecticides and the optimal timing of insecticide application on populations [23]. Therefore, we develop a new improved model based on the one proposed by Ali [15]. Let N_t and Q_t represent the larch budmoth density and plant mass at time t, respectively. This model assumes a specific season of length one, during which an individual acquires energy for reproduction. In this study, we alternate this season with the reproductive season. Insecticides are sprayed at some time $\theta(0 < \theta < 1)$ during the season, and the population growth depends on N_t and pN_t [24] before and after θ, respectively. We suppose that the dynamical behavior of the larch budmoth population is controlled by the Ricker equation $N_{t+1} = N_t e^{-\frac{rN_t}{k}}$, where the source of food affects the larch budmoth population through the moth's intrinsic growth rate r [16], and k is the carrying capacity. The model is given by

$$\begin{cases} N_{t+1} = pN_t(\theta e^{r(Q_t - \frac{N_t}{k})} + (1-\theta)e^{r(Q_t - \frac{pN_t}{k})}) \\ Q_{t+1} = (1-b) + bQ_t - \theta\frac{cN_t}{d+N_t} - (1-\theta)\frac{cpN_t}{d+pN_t} \end{cases} \quad (1)$$

Where $t = 0, 1, 2, ..., p(0 \leq p \leq 1)$ is the residual rate of the pesticide, and c is the maximum ingestion rate and d is the half-saturation constant for the larch budmoth population. Furthermore, $(1-b)$ is the plant quality recovery rate, and the plant quality will decay to 0 at the rate of b if the plant is unable to renew itself.It is important to note that all parameters should be greater than 0 to ensure that the model makes sense, and $0 < b < 1$. The condition $c+b < 1$ must hold in order to ensure that the solution of system (1) is non-negative.

On the basis of an updated model of the interaction between the larch budmoth and plant quality, the goal of this

Manuscript received November 19, 2021; revised March 7, 2022. This work was supported by The National Natural Science Foundation of China under Grant 11961024.

Xiaohua Ren is a master student of School of Mathematics and Statistics, Hubei Minzu University, Enshi 445000, China (e-mail: 202030341@hbmzu.edu.cn).

Changcheng Xiang is a professor of School of Mathematics and Statistics, Hubei Minzu University, Enshi 445000, China (corresponding author to provide e-mail: xcc7426681@126.com).

Yi Yang is an associate professor of College of Computer Science and Engineering, Chongqing Three Gorges University, Chongqing 404020, China (corresponding author to provide e-mail: yang1595@126.com).

study is to theoretically analyze the existence and stability of positive fixed points in system (1). Subsequently, we analyze the existence of the period-doubling bifurcation and the Neimark-Sacker bifurcation using the center manifold theorem and bifurcation theory, and discuss the effects of insecticides under different conditions. Finally, our theoretical results are proven via numerical simulations.

II. Existence of positive fixed point

For system (1), let $N_t = N_{t+1} = N^*$ and $Q_t = Q_{t+1} = Q^*$. Then, the fixed point $E^* = (N^*, Q^*)$ satisfies the following equation :

$$\begin{cases} N^* = pN^*(\theta e^{r(Q^*-\frac{N^*}{k})} + (1-\theta)e^{r(Q^*-\frac{pN^*}{k})}) \\ Q^* = (1-b) + bQ^* - \theta\frac{cN^*}{d+N^*} - (1-\theta)\frac{cpN^*}{d+pN^*} \end{cases} \tag{2}$$

Clearly, system (1) always has a minutely fixed point $E_0 = (0,1)$ at which the larch budmoth becomes extinct. For the existence of an internal positive fixed point $E^* = (N^*, Q^*)$, we consider the following equation

$$\begin{cases} 1 = p(\theta e^{r(Q^*-\frac{N^*}{k})} + (1-\theta)e^{r(Q^*-\frac{pN^*}{k})}) \\ Q^* = 1-\sigma-\varsigma \end{cases} \tag{3}$$

where $\sigma = \frac{c\theta N^*}{(d+N^*)(1-b)}$ and $\varsigma = \frac{cp(1-\theta)N^*}{(d+pN^*)(1-b)}$.

Combining the two equations in (3), we can obtain

$$p\theta e^{r(1-\sigma-\varsigma-\frac{N^*}{k})} = 1 - p(1-\theta)e^{r(1-\sigma-\varsigma-\frac{pN^*}{k})}.$$

Define two auxiliary functions

$$\begin{cases} F(N^*) = p\theta e^{r(1-\sigma-\varsigma-\frac{N^*}{k})} \\ G(N^*) = 1 - p(1-\theta)e^{r(1-\sigma-\varsigma-\frac{pN^*}{k})} \end{cases} \tag{4}$$

The derivatives of system (4) are

$$\begin{cases} F'(N) = p\theta r(-\sigma-\varsigma-\frac{1}{k})e^{r(1-\sigma-\varsigma-\frac{N^*}{k})} \\ G'(N) = -p(1-\theta)r(-\frac{\sigma d}{(d+N^*)N^*} \\ -\frac{\sigma d}{(d+pN^*)N^*} - \frac{p}{k})e^{r(1-\sigma-\varsigma-\frac{pN^*}{k})} \end{cases} \tag{5}$$

where $\sigma = \frac{c\theta N^*}{(d+N^*)(1-b)}$ and $\varsigma = \frac{cp(1-\theta)N^*}{(d+pN^*)(1-b)}$.

It is obvious that $F'(N^*) < 0$ and $G'(N^*) > 0$. Hence, $F(N^*)$ is monotonically decreasing and $G(N^*)$ is monotonically increasing. Furthermore, owing to $\lim\limits_{N^*\to 0^+} Q^* = 1$, $\lim\limits_{N^*\to\infty} Q^* = 0$, and $1-b+bQ_t-c < Q_{t+1} < 1-b+bQ_t$, it follows that the Q-component of the solutions of system (1) satisfies

$$0 < \frac{1-b-c}{1-b} \leq \lim_{t\to\infty}\inf Q_t \leq \lim_{t\to\infty} Q_t \leq 1.$$

By calculation we can obtain $\lim\limits_{N\to 0^+} F(N) - G(N) = pe^r - 1$, $\lim\limits_{N\to\infty} F(N) - G(N) = -1$. Since $pe^r > 0$ holds constant, system (1) has a constant positive fixed point. To show the presence of an internal positive fixed point, we have carried out the numerical simulation shown in Fig. 1.

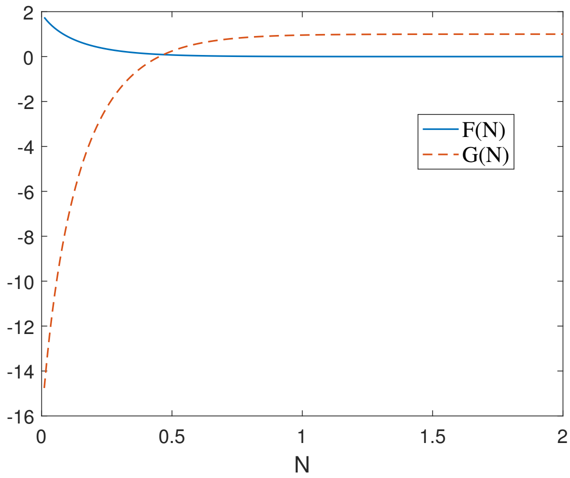

Fig. 1: Existence of the equilibrium $E^* = (N^*, Q^*)$ of system (1). The parameters are fixed as $c = 0.1$, $d = 0.1$, $b = 0.1$, $k = 0.5$, $p = 0.95$, $\theta = 0.1$, $r = 3$.

III. Mathematical analysis for the system

First, we calculate the Jacobian matrix of system (1) at $E^* = (N^*, Q^*)$ as

$$J(N^*,Q^*) = \begin{bmatrix} 1 - \frac{N^*rf+pN^*rg}{k} & N^*r \\ -\frac{c\theta d}{(d+N^*)^2} - \frac{c(1-\theta)pN^*}{(d+pN^*)^2} & b \end{bmatrix} \tag{6}$$

where $f = p\theta e^{r(Q_t-\frac{N_t}{k})}$, $\quad g = p(1-\theta)e^{r(Q_t-\frac{pN_t}{k})}$.

Hence, the characteristic polynomial is as follows:

$$\begin{aligned} P(\lambda) = \lambda^2 - (\frac{k-N^*rf-pN^*rg+kb}{k})\lambda \\ + \frac{(N^*+d)^2(pN^*+d)^2kb+\Gamma}{k(N^*+d)^2(pN^*+d)^2}, \end{aligned} \tag{7}$$

where

$$\begin{aligned} \Gamma = kc\theta dN^*r(pN^*+d)^2 + kc(1-\theta)pN^{*2}r \\ *(N^*+d)^2 - (N^*+d)^2(N^*rf+pN^*rg) \\ *(pN^*+d)^2b. \end{aligned}$$

From previous studies [25]–[27], we obtain Lemma 3.1 and Lemma 3.2 to analyze the stability conditions of system (1) at E^*.

Lemma 3.1. *Assume that $F(\lambda) = \lambda^2 - A\lambda + B$, if $F(1) > 0$ and λ_1, λ_2 are roots of $F(\lambda) = 0$. Then, the following statements hold:*

1. $|\lambda_1| < 1$ and $|\lambda_2| < 1$, if and only if $F(-1) > 0$ and $B < 1$.

2. $|\lambda_1| < 1$ and $|\lambda_2| > 1$, or $|\lambda_1| > 1$ and $|\lambda_2| < 1$ if and only if $F(-1) < 0$.

3. $|\lambda_1| < 1$ and $|\lambda_2| < 1$ if and only if $F(-1) > 0$ and $B > 1$.

4. $\lambda_1 = 1$ and $\lambda_2 \neq 1$ if and only if $F(-1) = 0$ and $B \neq 0, 2$.

5. λ_1 and λ_2 are complex and $|\lambda_1| = 1$ and $|\lambda_2| = 1$ if and only if $A^2 - 4B < 0$ and $B = 1$.

Let λ_1 and λ_2 be the eigenvalues of $J(N^*, Q^*)$ for system (1). We can review the relationship between the stability and the eigenvalues of the equilibrium states of two-dimensional systems. The unique positive fixed point E^* of system (1) is known as a locally asymptotically stable fixed sink if $|\lambda_1| < 1$ and $|\lambda_2| < 1$. E^* is called a source if $|\lambda_{1,2}| > 1$, and the source is unstable. E^* is called a saddle point if $|\lambda_1| < 1$ and $|\lambda_2| > 1$, or $|\lambda_1| > 1$ and $|\lambda_2| < 1$, and the saddle point is always unstable. E^* is called a nonhyperbolic point if either $|\lambda_1| = 1$ or $|\lambda_2| = 1$.

Next, the Jury condition is introduced so that we can identify the necessary and sufficient conditions for the eigenvalues of $J(N^*, Q^*)$ of system (1) to be greater or less than one [28], [29].

Lemma 3.2. *[Jury condition]: For the equation*

$$\lambda^2 + a_1\lambda + a_0 = 0, \tag{8}$$

where a_1 and a_0 are real numbers. Then :

1. A necessary and sufficient condition for both roots of (8) to have absolute values less than one is

$$a_1 < 1 + a_0 < 2.$$

2. A necessary and sufficient condition for both roots of (8) to have one absolute value greater than one and the other less than one is

$${a_1}^2 - 4a_0 > 0, \quad and \quad a_1 > 1 + a_0.$$

3. A necessary and sufficient condition for the absolute value of both roots of (8) to be greater than one is

$$a_0 > 1, \quad and \quad a_1 < 1 + a_0.$$

Theorem 3.1. *Assume that $E^* = (N^*, Q^*)$ is a unique positive fixed point of system (1). Then, the following conditions hold:*

1. E^* is a source if and only if

$$\begin{aligned} &\left|(N^*+d)^2(pN^*+d)^2kb+\Gamma\right| \\ &> \left|k(N^*+d)^2(pN^*+d)^2\right|, \end{aligned}$$

and

$$\begin{aligned} &\left|\frac{k-N^*rf-pN^*rg+kb}{k}\right| \\ &< \left|1+\frac{(N^*+d)^2(pN^*+d)^2kb+\Gamma}{k(N^*+d)^2(pN^*+d)^2}\right|. \end{aligned}$$

2. E^* is a saddle point if and only if

$$\begin{aligned} &(k-N^*rf-pN^*rg+kb)^2(N^*+d)^2 \\ &*(pN^*+d)^2k > 4k^2((N^*+d)^2(pN^*+d)^2kb \\ &+\Gamma), \end{aligned}$$

and

$$\begin{aligned} &\left|\frac{k-N^*rf-pN^*rg+kb}{k}\right| \\ &> \left|1+\frac{(N^*+d)^2(pN^*+d)^2kb+\Gamma}{k(N^*+d)^2(pN^*+d)^2}\right|. \end{aligned}$$

3. E^* is a nonhyperbolic point if and only if

$$\begin{aligned} &\left|\frac{k-N^*rf-pN^*rg+kb}{k}\right| \\ &= \left|1+\frac{(N^*+d)^2(pN^*+d)^2kb+\Gamma}{k(N^*+d)^2(pN^*+d)^2}\right|, \end{aligned} \tag{9}$$

and

$$\left|\frac{k-N^*rf-pN^*rg+kb}{k}\right| \le 2, \tag{10}$$

where $f = p\theta e^{r(Q_t - \frac{N_t}{k})}$, $g = p(1-\theta)e^{r(Q_t - \frac{pN_t}{k})}$,
$\Gamma = kc\theta dN^*r(pN^*+d)^2 + kc(1-\theta)pN^{*2}r(N^*+d)^2 - (N^*+d)^2(N^*rf + pN^*rg)(pN^*+d)^2b$.

Lemma 3.3. *If both equations (9) and (10) are not satisfied, the unique positive fixed point of system (1) is locally asymptotically stable if and only if*

$$\begin{aligned} &\frac{k-N^*rf-pN^*rg+kb}{k} \\ &< 1+\frac{(N^*+d)^2(pN^*+d)^2kb+\Gamma}{k(N^*+d)^2(pN^*+d)^2} < 2. \end{aligned}$$

A necessary and sufficient condition for the local asymptotic stability of the unique positive fixed point N^* of system (1) is given in Lemma 3.3.

IV. Bifurcation analysis

Referring to previous studies, we investigate period-doubling bifurcation and the Neimark-Sacker bifurcation using the central manifold theorem and divergence theory [26], [27].

A. Period-doubling bifurcation

This bifurcation process is a typical path to chaos and can be regarded as a way of entering chaos from the periodic window. As the precondition for period-doubling bifurcation to occur is for a nonhyperbolic fixed point in system (1), it follows from the previous theoretical analysis that a nonhyperbolic fixed point occurs if and only if the two characteristic roots of the characteristic equation for system (1) satisfy $\lambda_1 = -1$ and $\lambda_2 \neq 1$. Thus we obtain the associated parametric conditions. Rewrite the characteristic polynomial of system (1) at $E^* = (N^*, Q^*)$ as

$$F(\lambda) = \lambda^2 - A\lambda + B, \tag{11}$$

where $A = \frac{k-N^*rf-pN^*rg+kb}{k}$, and $B = \frac{(N^*+d)^2(pN^*+d)^2kb+\Gamma}{k(N^*+d)^2(pN^*+d)^2}$.

Assuming that $A^2 > 4B$, we get

$$\begin{aligned} &(\frac{k-N^*rf-pN^*rg+kb}{k})^2 \\ &> 4\frac{(N^*+d)^2(pN^*+d)^2kb+\Gamma}{k(N^*+d)^2(pN^*+d)^2}, \end{aligned}$$

and assuming that $A + B = -1$, we get

$$\begin{aligned} &\frac{k-N^*rf-pN^*rg+kb}{k} \\ &+\frac{(N^*+d)^2(pN^*+d)^2kb+\Gamma}{k(N^*+d)^2(pN^*+d)^2} = -1. \end{aligned}$$

Moreover, as one of the roots of $F(\lambda) = 0$ is $\lambda_1 = -1$, we can obtain the other root as $\lambda_2 = -B$. Owing to $\lambda_2 \neq 1$, this means that

$$\frac{(N^*+d)^2(pN^*+d)^2kb+\Gamma}{k(N^*+d)^2(pN^*+d)^2} \neq \pm 1.$$

Considering the analysis presented above, system (1) involves period-doubling bifurcation at $E^* = (N^*, Q^*)$ when the parameters satisfying the above-mentioned conditions are perturbed within a small range.

Next, let us write p as p_1, and with the addition of the small perturbation parameter $\bar{p}$, the following two-dimensional mapping can be used to define system (1) :

$$\begin{pmatrix} N \\ Q \end{pmatrix} \rightarrow \begin{pmatrix} \Psi_1 \\ \Phi_1 \end{pmatrix} \tag{12}$$

where

$\Psi_1 = (p_1+\bar{p})N(\theta e^{r(Q-\frac{N}{k})} + (1-\theta)e^{r(Q-\frac{(p_1+\bar{p})N}{k})})$

$\Phi_1 = (1-b) + bQ - \theta\frac{cN}{d+N} - (1-\theta)\frac{c(p_1+\bar{p})N}{d+pN}$

The small perturbation parameter $\bar{p} \lll 1$. Take $x = N - N^*$ and $y = Q - Q^*$ to change the unique positive fixed point $E^* = (N^*, Q^*)$ toward the origin; then, map (13) is put into the following format:

$$\begin{pmatrix} x \\ y \end{pmatrix} \rightarrow \begin{pmatrix} a_{11} & a_{12} \\ a_{21} & a_{22} \end{pmatrix}\begin{pmatrix} x \\ y \end{pmatrix} + \begin{pmatrix} h(x,y,\bar{r}) \\ j(x,y,\bar{r}) \end{pmatrix}, \tag{13}$$

where

$$\begin{aligned} h(x,y,\bar{p}) &= a_{13}x^2 + a_{14}xy + a_{15}y^2 + b_1x^3 \\ &\quad + b_2x^2y + b_3xy^2 + b_4y^3 + e_1\bar{p}x + e_2\bar{p}y \\ &\quad + e_3\bar{p}xy + e_4\bar{p}y^2 + e_5\bar{p}x^2 \\ &\quad + O\left((|x|+|y|+|\bar{p}|)^4\right), \\ j(x,y,\bar{p}) &= a_{23}x^2 + a_{24}x^3 + O\left((|x|+|y|+|\bar{p}|)^4\right). \end{aligned}$$

$$a_{11} = 1 - \frac{\mathrm{N}^*r\mathrm{f} + \mathrm{p}_1\ \mathrm{N}^*r\mathrm{g}}{\mathrm{k}}, \quad a_{12} = \mathrm{N}^*r,$$

$$a_{13} = \frac{\mathrm{N}^*r^2\mathrm{f} + \mathrm{N}^*r^2\mathrm{p}_1^2\ \mathrm{g} - 2\mathrm{k}r\mathrm{f} - 2\mathrm{kp}_1r\mathrm{g}}{2k^2},$$

$$a_{14} = \frac{\mathrm{kr} + \mathrm{r}^2\ \mathrm{N}^*\mathrm{f} - \mathrm{r}^2\ \mathrm{N}^*\mathrm{p}_1\ \mathrm{g}}{\mathrm{k}}, \quad a_{15} = \frac{\mathrm{r}^2\ \mathrm{N}^*}{2},$$

$$b_1 = \frac{3kr^2f + 3kr^2p_1^2g + N^*r^3f - N^*r^3p_1^3g}{6k^3},$$

$$b_2 = \frac{\mathrm{N}^*\mathrm{r}^3\mathrm{f} + \mathrm{N}^*\mathrm{r}^3\mathrm{p}_1{}^2\ \mathrm{g} - 2k\mathrm{r}^2\mathrm{f} - 2\mathrm{kr}^2\mathrm{p}_1\ \mathrm{g}}{2k^2},$$

$$b_3 = \frac{\mathrm{kr}^2 + \mathrm{N}^*\mathrm{r}^3\mathrm{f} - \mathrm{N}^*\mathrm{r}^3\mathrm{p}_1\ \mathrm{g}}{2k}, \quad b_4 = \frac{\mathrm{N}^*\mathrm{r}^3}{6},$$

$$e_1 = \frac{k^2 - 3kp_1rN^*g - N^*krf + p_1{}^2r^2N^{*2}g}{k^2p_1},$$

$$e_2 = \frac{N^*rk - N^{*2}r^2p_1g}{kp_1},$$

$$e_3 = \frac{k^2r - 3p_1kN^*r^2g - N^*r^2kf + p_1{}^2N^{*2}r^3g}{k^2p_1},$$

$$\mathrm{e}_4 = \frac{N^*r^2k - N^{*2}r^3p_1g}{2p_1k}, e_5 = \frac{\varpi}{2p_1k^3},$$

where

$$\begin{aligned} \varpi &= kN^*r^2f + p_1{}^2kN^*r^2g + 4p_1{}^2kN^*r^2g \\ &\quad - 2k^2rf - 4p_1k^2rg - p_1{}^3N^3r^3g \end{aligned}$$

$$a_{21} = -\frac{c\theta d}{(d+N^*)^2} - \frac{c(1-\theta)pN^*}{(d+pN^*)^2}, \quad a_{22} = b,$$

$$a_{23} = \frac{c\theta d}{(d+N^*)^3} + \frac{c(1-\theta)pN^*}{(d+pN^*)^3},$$

$$a_{24} = -\frac{c\theta d}{(d+N^*)^4} - \frac{c(1-\theta)pN^*}{(d+pN^*)^4}.$$

The next step is to angularize system (13) according to the conversion T.

$$\begin{pmatrix} x \\ y \end{pmatrix} = T\begin{pmatrix} u \\ v \end{pmatrix}, \tag{14}$$

where $\mathrm{T} = \begin{pmatrix} \mathrm{a}_{12} & \mathrm{a}_{12} \\ -1-\mathrm{a}_{11} & \lambda_2 - \mathrm{a}_{11} \end{pmatrix}$ is a nonsingular matrix. As a result of conversion (14), map (13) can be represented as

$$\begin{pmatrix} u \\ v \end{pmatrix} \rightarrow \begin{pmatrix} -1 & 0 \\ 0 & \lambda_2 \end{pmatrix}\begin{pmatrix} u \\ v \end{pmatrix} + \begin{pmatrix} h(u,v,\bar{p}) \\ j(u,v,\bar{p}) \end{pmatrix}, \tag{15}$$

where

$$\begin{aligned} h(u,v,\bar{p}) &= \left(\frac{a_{13}(\lambda_2 - a_{11})}{a_{12}(\lambda_2+1)} - \frac{a_{23}}{\lambda_2+1}\right)x^2 \\ &+ \frac{a_{14}(\lambda_2 - a_{11})}{a_{12}(\lambda_2+1)}xy + \frac{a_{15}(\lambda_2 - a_{11})}{a_{12}(\lambda_2+1)}y^2 \\ &+ \left(\frac{b_1(\lambda_2 - a_{11})}{a_{12}(\lambda_2+1)}\frac{a_{24}}{\lambda_2+1}\right)x^3 + \frac{b_2(\lambda_2 - a_{11})}{a_{12}(\lambda_2+1)}x^2y \\ &+ \frac{b_3(\lambda_2 - a_{11})}{a_{12}(\lambda_2+1)}xy^2 + \frac{b_4\left(\frac{\lambda}{2} - a_{11}\right)}{a_{12}(\lambda_2+1)}y^3 \\ &+ \frac{e_1\left(\frac{\lambda}{2} - a_{11}\right)}{a_{12}(\lambda_2+1)}\bar{p}x + \frac{e_2\left({}^{\lambda}{}_2 - a_{11}\right)}{a_{12}(\lambda_2+1)}\bar{p}y \\ &+ \frac{e_3\left({}^{\lambda}{}_2 - a_{11}\right)}{a_{12}(\lambda_2+1)}\bar{p}xy + \frac{e_4\left({}^{\lambda}{}_2 - a_{11}\right)}{a_{12}(\lambda_2+1)}\bar{p}y^2 \\ &+ \frac{e_5(\lambda_2 - a_{11})}{a_{12}(\lambda_2+1)}\bar{p}x^2 + o\left((u+v+\bar{p})^4\right), \end{aligned}$$

$$\begin{aligned} j(u,v,\bar{p}) &= \left(\frac{a_{13}(1+a_{11})}{a_{12}(\lambda_2+1)} - \frac{a_{23}}{\lambda_2+1}\right)x^2 \\ &+ \frac{a_{14}(1+a_{11})}{a_{12}(\lambda_2+1)}xy + \frac{a_{15}(1+a_{11})}{a_{12}(\lambda_2+1)}y^2 \\ &+ \left(\frac{b_1(1+a_{11})}{a_{12}(\lambda_2+1)} + \frac{a_{24}}{\lambda_2+1}\right)x^3 \\ &+ \frac{b_2(1+a_{11})}{a_{12}({}^{\lambda}{}_2+1)}x^2y + \frac{b_3(1+a_{11})}{a_{12}({}^{\lambda}{}_2+1)}xy^2 \\ &+ \frac{b_4(1+a_{11})}{a_{12}(\lambda_2+1)}y^3 + \frac{e_1(1+a_{11})}{a_{12}({}^{\lambda}{}_2+1)}\bar{p}x \\ &+ \frac{e_2(1+a_{11})}{a_{12}({}^{\lambda}{}_2+1)}\bar{p}y + \frac{e_3(1+a_{11})}{a_{12}(\lambda_2+1)}\bar{p}xy \\ &+ \frac{e_4(1+a_{11})}{a_{12}(\lambda_2+1)}\bar{p}y^2 + \frac{e_5(1+a_{11})}{a_{12}(\lambda_2+1)}\bar{p}x^2 \\ &+ o\left((u+v+\bar{p})^4\right), \end{aligned}$$

where $x = a_{12}(u+v)$ and $y = -(1+a_{11})u + (\lambda_2 - a_{11})v$.

The central manifold theorem has important applications in bifurcation theory. We use the central manifold theorem of system (15) to approve the central manifold at the origin, based on parameter p_1. Depending on the center manifold theorem, for parameter values around $\bar{p} = 0$, the behavior of map (13) surrounding the fixed point (0, 0) can be studied using the single parameter map family on the central manifold [30].

The central manifold is determined in a small neighbourhood of $\bar{p} = 0$ as

$$W^c = \left\{(u,v,\bar{p}) \in IR^3 : s_2(u,\bar{p}), s_2(0,0) = Ds_2(0,0) = 0\right\}.$$

The central manifold is in tangency to the $v = 0$ axes, as understood from the equation above. Suppose that $S_2(u, \bar{p})$ can be written as

$$s_2(u, \bar{p}) = m_1 u^2 + m_2 u\bar{p} + m_3 \bar{p}^2 + O\left((u + \bar{p})^3\right), \quad (16)$$

where

$$m_1 = \frac{\Lambda}{a_{12}(\lambda_2 - 1)^2},$$

$$m_2 = \frac{(1 + a_{11})(-a_{12}e_1 + e_2 + a_{11}e_2)}{a_{12}(\lambda_2 + 1)^2},$$

$$m_3 = 0.$$

where $\Lambda = (1+a_{11})a_{12}^2 a_{13} - (1+a_{11})^2 a_{12}a_{14} + (1+a_{11})^3 a_{15} + a_{12}^3 a_{23}$

Restricting map (15) to the central manifold $W^c(0, 0, 0)$ gives

$$\begin{aligned} F: u \to & -u + \rho_1 u^2 + \rho_2 u\bar{p} + \rho_3 u^2\bar{p} + \rho_4 u\bar{p}^2 \\ & + \rho_5 u^3 + O\left((u + \bar{p})^4\right), \end{aligned} \quad (17)$$

where $\rho_1, \rho_2, \rho_3, \rho_4$, and ρ_5 are coefficients.

$$\begin{aligned}
\rho_1 =& \frac{1}{a_{12}(\lambda_2 + 1)}[((\lambda_2 - a_{11})a_{13} - a_{12}a_{23})a_{12}{}^2 \\
& - a_{12}a_{14}(a_{11} - \lambda_2)(-1 - a_{11}) \\
& - a_{15}(-1 - a_{11})^2(a_{11} - \lambda_2)], \\
\rho_2 =& \frac{(a_{11} - \lambda_2)(e_1 a_{12} - e_2(-1 - a_{11}))}{a_{12}(\lambda_2 + 1)} \\
\rho_3 =& 2(\frac{(\lambda_2 - a_{11})a_{13} - a_{12}a_{23}}{a_{12}(\lambda_2 + 1)})a_{12}{}^2 m_2 \\
& + \frac{(\lambda_2 - a_{11})}{a_{12}(\lambda_2 + 1)}[a_{12}{}^2 e_5 + a_{12}e_1 m_1 \\
& + (\lambda_2 - a_{11})(e_2 m_1 + a_{12}a_{14}m_2) \\
& + (-1 - a_{11})(a_{12}e_3 + a_{14}m_2) \\
& + (-1 - a_{11})e_4 + (\lambda_2 - a_{11})2m_2 a_{15})], \\
\rho_4 =& 2(\frac{(\lambda_2 - a_{11})a_{13} - a_{12}a_{23}}{a_{12}(\lambda_2 + 1)})a_{12}{}^2 m_3 \\
& + \frac{(\lambda_2 - a_{11})}{a_{12}(\lambda_2 + 1)}[a_{12}e_1 m_1 + (\lambda_2 - a_{11}) \\
& * (e_2 m_2 + a_{12}a_{14}m_3) + (-1 - a_{11}) \\
& * (a_{12}a_{14}m_3 + (\lambda_2 - a_{11})2m_3 a_{15})], \\
\rho_5 =& 2(\frac{(\lambda_2 - a_{11})a_{13} - a_{12}a_{23}}{a_{12}(\lambda_2 + 1)})a_{12}{}^2 m_1 \\
& + (\frac{(\lambda_2 - a_{11})b_1 - a_{12}a_{24}}{a_{12}(\lambda_2 + 1)})a_{12}{}^3 \\
& + \frac{(\lambda_2 - a_{11})}{a_{12}(\lambda_2 + 1)}[(-1 - a_{11}) \\
& * (a_{12}{}^2 b_2 + a_{12}a_{14}m_1) + (\lambda_2 - a_{11}) \\
& * (2m_1 a_{15}(-1 - a_{11}) + a_{12}a_{14}m_1) \\
& + a_{12}b_3(-1 - a_{11})^2 + b_4(-1 - a_{11})^3].
\end{aligned}$$

Let

$$\alpha_1 = \left(\frac{\partial^2 f}{\partial u \partial \bar{p}} + \frac{1}{2}\frac{\partial F}{\partial \bar{p}}\frac{\partial^2 F}{\partial u^2}\right)_{(0,0)},$$

$$\alpha_2 = \left(\frac{1}{6}\frac{\partial^3 F}{\partial u^3} + \left(\frac{1}{2}\frac{\partial^2 F}{\partial u^2}\right)^2\right)_{(0,0)}.$$

The previous analysis [31] gives Theorem 4.1, which summarizes the conditions for the occurrence of a period-doubling bifurcation in system (1).

Theorem4.1. *In the case of $\alpha_1 \neq 0$ and $\alpha_2 \neq 0$, system (1) involves a period-doubling bifurcation at the point $E^* = (N^*, Q^*)$ as the parameter p changes in a sufficiently small neighbourhood of p_1. Furthermore, if $\alpha_2 > 0$ $(\alpha_2 < 0)$, then the period-two orbits that bifurcate from (N^*, Q^*) are stable (unstable).*

B. Neimark-Sacker bifurcation

Here, we determine the survival conditions for the Neimark-Sacker bifurcation using bifurcation theory [30]. We know that the bifurcation of the system is called torus bifurcation or NS when the eigenvalue $\lambda_{1,2} = e^{\pm i\theta}$. We know that a sufficient necessary condition for a hyperbolic immobility point is to have a pair of complex conjugate eigenvalues of modulo 1.

The characteristic polynomial for system (1) at $E^* = (N^*, Q^*)$ is again written as :

$$F(\lambda) = \lambda^2 - A\lambda + B, \quad (18)$$

where $A = \frac{k - N^*rf - pN^*rg + kb}{k}$ and $B = \frac{(N^*+d)^2(pN^*+d)^2kb + \Gamma}{k(N^*+d)^2(pN^*+d)^2}$.

From Lemma 3.1, if the two roots of $F(\lambda) = 0$ are to be conjugate complex roots modulus 1, the following requirements must be satisfied :

$$B = 1 \quad and \quad A < 2.$$

Then, we can obtain

$$\frac{(N^* + d)^2(pN^* + d)^2 kb + \Gamma}{k(N^* + d)^2(pN^* + d)^2} = 1,$$
$$-N^*rf - pN^*rg + kb < k.$$

Considering the analysis presented above, system (1) involves the Neimark-Sacker bifurcation at $E^* = (N^*, Q^*)$ when the parameters satisfying the above-mentioned conditions are perturbed within a small range.

Next, let us write p as p_2, and with the addition of the small perturbation parameter $\bar{p}$, the following two-dimensional mapping can be used to define system (1):

$$\begin{pmatrix} N \\ Q \end{pmatrix} \to \begin{pmatrix} \Psi_2 \\ \Phi_2 \end{pmatrix} \quad (19)$$

where

$\Psi_2 = (p_2 + \bar{p})N(\theta e^{r(Q - \frac{N}{k})} + (1 - \theta)e^{r(Q - \frac{(p_2 + \bar{p})N}{k})})$

$\Phi_2 = (1 - b) + bQ - \theta\frac{cN}{d+N} - (1 - \theta)\frac{c(p_2 + \bar{p})N}{d+pN}$

The small perturbation parameter $\bar{p} \lll 1$. Take $x = N - N^*$ and $y = Q - Q^*$ to change $E^* = (N^*, Q^*)$ toward the origin; then, map (19) is put into the following format:

$$\begin{pmatrix} x \\ y \end{pmatrix} \to \begin{pmatrix} a_{11} & a_{12} \\ a_{21} & a_{22} \end{pmatrix}\begin{pmatrix} x \\ y \end{pmatrix} + \begin{pmatrix} h(x, y) \\ j(x, y) \end{pmatrix}, \quad (20)$$

where

$h(x, y) = a_{13}x^2 + a_{14}xy + a_{15}y^2 + b_1x^3 + b_2x^2y + b_3xy^2 + b_4y^3 + O\left((|x| + |y| + |\bar{p}|)^4\right)$,

$j(x, y) = a_{23}x^2 + a_{24}x^3 + O\left((|x| + |y| + |\bar{p}|)^4\right)$.

Furthermore, the coefficients a_{11}, a_{12}, a_{13}, a_{14}, a_{15}, b_1, b_2, b_3, b_4, a_{21}, a_{22}, a_{23} and a_{24} are given by (13) by substituting p_1 for $p_2 + \bar{r}$. The equation of characteristics associated with system (20) assessed at (0, 0) is provided by the following equation

$$F(\lambda) = \lambda^2 - A(\bar{p})\lambda + B(\bar{p}) = 0, \quad (21)$$

where

$A(\bar{p}) = \frac{k-N^*rf-(p_2+\bar{p})N^*rg+kb}{k}$,

$B(\bar{p}) = \frac{(N^*+d)^2((p_2+\bar{p})N^*+d)^2kb+\Gamma(\bar{p})}{k(N^*+d)^2((p_2+\bar{p})N^*+d)^2}$,

$$\begin{aligned}\Gamma(\bar{p}) =& kc\theta dN^*r((p_2+\bar{p})N^*+d)^2\\ &+kc(1-\theta)(p_2+\bar{p})N^{*2}r(N^*+d)^2\\ &-(N^*+d)^2(N^*rf+(p_2+\bar{p})N^*rg)\\ &*((p_2+\bar{p})N^*+d)^2b\ .\end{aligned}$$

Because of the existence of a pair of complex conjugates λ_1, λ_2, where $\lambda_2=\overline{\lambda_1}$ and $|\lambda_1|=|\lambda_2|=1$ for the eigenvalues of (0, 0), we have

$$\lambda_1,\lambda_2 = \frac{A(\bar{p})}{2} \pm \frac{i}{2}\sqrt{4B(\bar{p})-A^2(\bar{p})}.$$

We obtain $|\lambda_1|=|\lambda_2|=\sqrt{B(\bar{p})}$, $\left(\frac{d\lambda}{d\bar{p}}\right)_{\bar{p}=0} = \left(\frac{d\lambda}{d\bar{p}}\right)_{\bar{p}=0} = \left(\frac{d\sqrt{B(\bar{p})}}{d\bar{p}}\right)_{\bar{p}=0} \neq 0$.

Furthermore, when $\bar{p}=0$, $\lambda_1^m,\lambda_2^m \neq 1$ for $m=1,2,3,4$, which is similar to $A(0)\neq -2,0,1,2$.

It follows that

$$-2 < A(0) = \frac{\mathrm{k}-\mathrm{N}^*r\mathrm{f}-\mathrm{p}_2\mathrm{N}^*r\mathrm{g}+\mathrm{kb}}{\mathrm{k}} < 2.$$

We also expect that $A(0)\neq 0,1$. This implies that

$$\left\{\begin{array}{l}\mathrm{N}^*r\mathrm{f}+\mathrm{p}_2\mathrm{N}^*r\mathrm{g}\neq \mathrm{kb}\\ \mathrm{k}+\mathrm{kb}\neq \mathrm{N}^*r\mathrm{f}+\mathrm{p}_2\mathrm{N}^*r\mathrm{g}\end{array}\right. . \tag{22}$$

Consequently, we get $A(0)\neq -2,0,1,2$ and $\lambda_1^m,\lambda_2^m\neq 1$ for all $m=1,2,3,4$ at $\bar{p}=0$. Therefore, when $\bar{p}=0$, the root from (21) at the origin (0, 0) is not at the point of intersection of the coordinate axis with the unit circle, while (22) holds.

To investigate the normal form of (20), we let $\alpha = \frac{\mathrm{A}(0)}{2}, \beta=\frac{1}{2}\sqrt{4\ \mathrm{B}(0)-\mathrm{A}^2(0)}$ when $\bar{p}=0$ and make the following conversions :

$$\begin{pmatrix} x\\ y\end{pmatrix} = T\begin{pmatrix} u\\ v\end{pmatrix}, \tag{23}$$

where $T=\begin{pmatrix} a_{12} & 0\\ \alpha-a_{11} & -\beta\end{pmatrix}$ is an invertible matrix. As a result of the (23), map (20) can be described as

$$\begin{pmatrix} u\\ v\end{pmatrix}\to\begin{pmatrix}\alpha & -\beta\\ \beta & \alpha\end{pmatrix}\begin{pmatrix} u\\ v\end{pmatrix}+\begin{pmatrix}\tilde{h}(u,v)\\ \tilde{\jmath}(u,v)\end{pmatrix}, \tag{24}$$

where

$$\begin{aligned}\tilde{h}(u,v) =& \frac{a_{13}}{a_{12}}x^2+\frac{a_{14}}{a_{12}}xy+\frac{a_{15}}{a_{12}}y^2+\frac{b_1}{a_{12}}x^3\\ &+\frac{b_2}{a_{12}}x^2y+\frac{b_3}{a_{12}}xy^2+\frac{b_4}{a_{12}}y^3\\ &+O\left((u+\bar{p})^4\right),\\ \tilde{\jmath}(u,v) =& \left(\frac{(\alpha-a_{11})\,a_{13}}{a_{12}\beta}-\frac{a_{23}}{\beta}\right)x^2\\ &+\frac{(\alpha-a_{11})\,a_{14}}{a_{12}\beta}xy+\frac{(\alpha-a_{11})\,a_{15}}{a_{12}\beta}y^2\\ &+\left(\frac{(\alpha-a_{11})\,b_1}{a_{12}\beta}-\frac{a_{24}}{\beta}\right)x^3\\ &+\frac{(\alpha-a_{11})\,b_2}{a_{12}\beta}x^2y+\frac{(\alpha-a_{11})\,b_3}{a_{12}\beta}xy^2\\ &+\frac{(\alpha-a_{11})\,b_4}{a_{12}\beta}y^3+O\left((u+\bar{p})^4\right)\ ,\end{aligned}$$

where $x=a_{12}u$ and $y=(\alpha-a_{11})u-\beta v$.

To determine whether the Neimark-Sacker bifurcation occurs in system (24), we need to verify it through the following conditions, i.e., $L\neq 0$.

$$\begin{aligned}\mathrm{L} =& -\mathrm{Re}\left(\frac{(1-2\lambda)\lambda^2}{1-\lambda}\zeta_{20}\zeta_{11}\right)-\frac{1}{2}\left|\zeta_{11}\right|^2\\ &-\left|\zeta_{02}\right|^2+\mathrm{Re}\left(\lambda\zeta_{21}\right),\end{aligned} \tag{25}$$

where

$$\begin{aligned}\zeta_{20} &= \tfrac{1}{8}\left(\tilde{\mathrm{h}}_{\mathrm{uu}}-\tilde{\mathrm{h}}_{\mathrm{vv}}+2\tilde{\mathrm{j}}_{\mathrm{uv}}+\mathrm{i}\left(\tilde{\mathrm{J}}_{\mathrm{uu}}-\tilde{\mathrm{j}}_{\mathrm{vv}}-2\tilde{\mathrm{h}}_{\mathrm{uv}}\right)\right),\\ \zeta_{11} &= \tfrac{1}{4}\left(\tilde{\mathrm{h}}_{\mathrm{uu}}+\tilde{\mathrm{h}}_{\mathrm{vv}}+\mathrm{i}\left(\tilde{\mathrm{J}}_{\mathrm{uu}}+\tilde{\mathrm{J}}_{\mathrm{vv}}\right)\right),\\ \zeta_{02} &= \tfrac{1}{8}\left(\tilde{\mathrm{h}}_{\mathrm{uu}}-\tilde{\mathrm{h}}_{\mathrm{vv}}-2\tilde{\mathrm{J}}_{\mathrm{uv}}+\mathrm{i}\left(\tilde{\mathrm{J}}_{\mathrm{uu}}-\tilde{\mathrm{J}}_{\mathrm{vv}}-2\tilde{\mathrm{h}}_{\mathrm{uv}}\right)\right),\\ \zeta_{21} &= \tfrac{1}{16}\left(\tilde{\mathrm{h}}_{\mathrm{uuu}}+\tilde{\mathrm{h}}_{\mathrm{vvv}}+\tilde{\mathrm{j}}_{\mathrm{uuv}}+\tilde{\mathrm{J}}_{\mathrm{vvv}}\right.\\ &\quad\left.+\mathrm{i}\left(\tilde{\mathrm{J}}_{\mathrm{uuu}}+\tilde{\mathrm{j}}_{\mathrm{uvv}}-\tilde{\mathrm{h}}_{\mathrm{uuv}}-\tilde{\mathrm{h}}_{\mathrm{vvv}}\right)\right),\end{aligned}$$

and

$$\begin{aligned}\tilde{h}_{uu} &= 2a_{12}a_{13}+2a_{14}\left(\alpha-a_{11}\right)+2\tfrac{a_{15}(\alpha-a_{11})^2}{a_{12}},\\ \tilde{h}_{vv} &= 2\beta^2\tfrac{a_{15}}{a_{12}},\\ \tilde{h}_{uv} &= -\beta a_{14}-2\beta\tfrac{a_{15}}{a_{12}},\\ \tilde{h}_{uuu} &= 6a_{12}^2b_1+6a_{12}\ b_2\left(\alpha-a_{11}\right)\\ &+6\ b_3\left(\alpha-a_{11}\right)^2+6\tfrac{b_4(\alpha-a_{11})^3}{a_{12}},\\ \tilde{h}_{uuv} &= -2a_{12}\ b_2\beta-4\ b_3\beta\left(\alpha-a_{11}\right)\\ &-6\tfrac{b_4\beta(\alpha-a_{11})^2}{a_{12}},\\ \tilde{h}_{uvv} &= 2a_{12}\ b_3\beta^2+6\tfrac{b_4\beta^2(\alpha-a_{11})}{a_{12}},\\ \tilde{h}_{vvv} &= -18\tfrac{a_{14}\beta^3}{a_{12}},\end{aligned}$$

$$\begin{aligned}\tilde{J}_{uu} &= 2a_{12}^2\left(\tfrac{a_{13}(\alpha-a_{11})}{a_{12}\beta}-\tfrac{a_{23}}{\beta}\right)+2\tfrac{a_{14}(\alpha-a_{11})^2}{\beta}\\ &+2\tfrac{a_{15}(\alpha-a_{11})^3}{a_{12}\beta},\\ \tilde{J}_{vv} &= 2\tfrac{a_{15}\beta(\alpha-a_{11})}{a_{12}},\\ \tilde{J}_{uv} &= -a_{14}\left(\alpha-a_{11}\right)-2\tfrac{a_{15}(\alpha-a_{11})^2}{a_{12}},\\ \tilde{J}_{uuu} &= 6{a_{12}}^3\left(\tfrac{b_1(\alpha-a_{11})}{a_{12}\beta}-\tfrac{a_{24}}{\beta}\right)\\ &+6\tfrac{a_{12}\ b_2(\alpha-a_{11})^2}{\beta}+6\tfrac{b_3(\alpha-a_{11})^3}{\beta}+6\tfrac{b_4(\alpha-a_{11})^4}{a_{12}\beta},\\ \tilde{J}_{uuv} &= -2a_{12}\ b_2\left(\alpha-a_{11}\right)-4\ b_3\left(\alpha-a_{11}\right)^2\\ &-6\tfrac{b_4(\alpha-a_{11})^3}{a_{12}},\\ \tilde{J}_{uvv} &= 2\ b_3\beta\left(\alpha-a_{11}\right)+6\tfrac{b_4\beta(\alpha-a_{11})^2}{a_{12}},\\ \tilde{J}_{vvv} &= -18\tfrac{b_4\beta^2(\alpha-a_{11})}{a_{12}}.\end{aligned}$$

Through the analysis presented above, we get Theorem 4.2.

Theorem 4.2. *If requirement (22) is established and $L\neq 0$, system (1) involves the Neimark-Sacker bifurcation at the point $E^*=(N^*,Q^*)$ as the parameter p_2 changes in a sufficiently small neighbourhood of $\bar{\mathrm{p}}$. Furthermore, if $L<0$ ($L>0$), then the invariant closed curve that bifurcates from $E^*=(N^*,Q^*)$ is attracting (repelling), which is also called the supercritical (subcritical) Neimark-Sacker bifurcation.*

V. Numerical simulation and discussion

A. Numerical bifurcation analysis

The theoretical bifurcation analysis described in the previous section indicated that system (1) involves period-doubling bifurcation and the Neimark-Sacker bifurcation

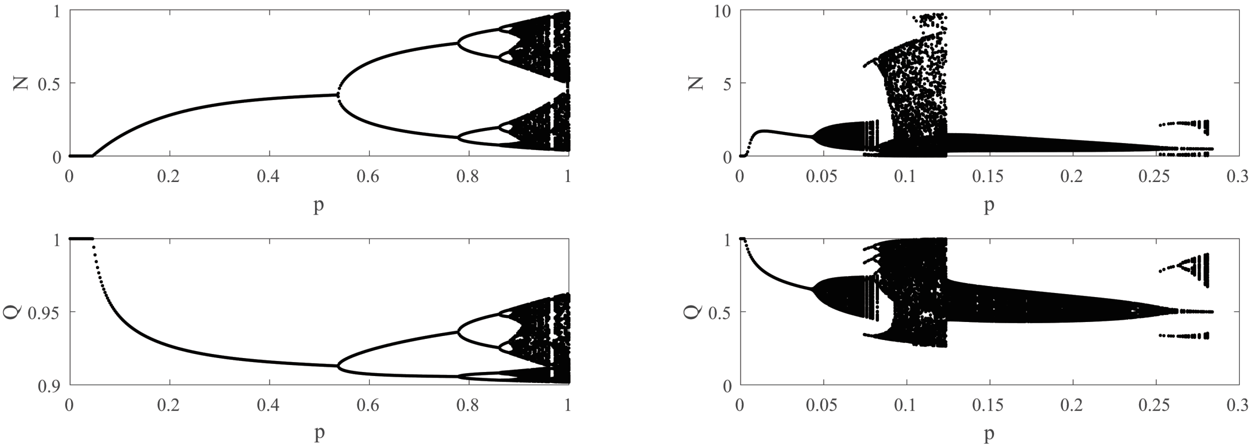

(a) (b)

Fig. 2: Period-doubling bifurcation diagram and Neimark-Sacker bifurcation diagram for system (1). $b = 0.1$, $c = 0.1$, $d = 0.1$, $k = 0.5$, $\theta = 0.8$, $r = 3.1$ in (a); $b = 0.1$, $c = 0.75$, $d = 0.1$, $k = 0.5$, $\theta = 0.1$, $r = 6$ in (b).

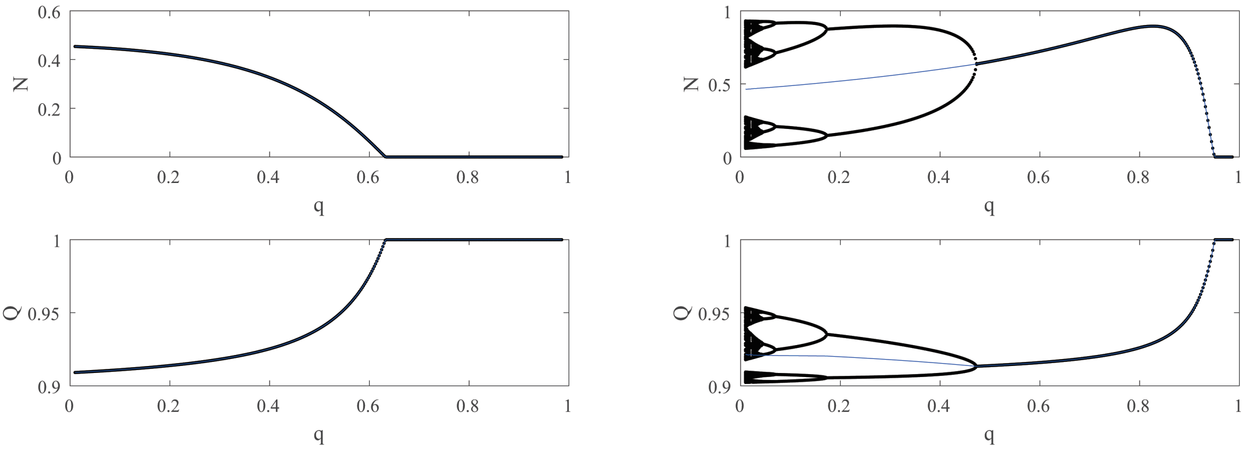

(a) r=1 (b) r=3

Fig. 3: Bifurcation diagrams of system (1) with respect to q for different values of r. The parameters $b = 0.1$, $c = 0.1$, $d = 0.1$, $k = 0.5$, $theta = 0.1$, blue line is the mean value.

when the residual rate p passes a certain critical value, indicating that small changes in insecticide mortality $q = 1 - p$ cause significant changes in moth density. We discuss the numerical bifurcation analysis below.

On the basis of the bifurcated flow shapes given in equations (17) and (25), two types of bifurcations can be simulated numerically, as shown in Fig. 3. In Fig. 3 (a), we fix the parameters $b = 0.1$, $c = 0.1$, $d = 0.1$, $k = 0.5$, $\theta = 0.8$, and $r = 3.1$, and these parameters satisfy the conditions for the occurrence of the period-doubling bifurcation of system (1). We can observe that the period-doubling bifurcation occurs from the unique fixed point $E = (N^*, Q^*) = (0.417, 0.931)$ at $p = 0.535$. In Fig. 3 (b), we fix the parameters $c = 0.75$, $d = 0.1$, $b = 0.1$, $k = 0.5$, $\theta = 0.1$, and $r = 6$, and these parameters satisfy the conditions for the occurrence of the Neimark-Sacker bifurcation of system (1). We can observe that the Neimark-Sacker bifurcation occurs from the unique fixed point $E = (N^*, Q^*) = (1.341, 0.66)$ at $p = 0.4$.

To conveniently observe the suppressive effect of the insecticide mortality q on high budmoth density, we will draw bifurcation diagrams of system (1) with respect to $q = 1 - p$. In Figure 3, the value of r is varied to observe the effect of the natural growth rate on the population size. When $r = 3$, an interesting phenomenon occurs; as the mortality rate q of the insecticide increases, the steady state of the moth density can continue to increase until it increases to a local value maximum, which demonstrates that as the insecticide efficiency increases, the moth density increases instead of decreasing; however, when $r = 1$, the steady state of moth density gradually decreases as the insecticide efficiency increases. Therefore, the natural growth rate of moths and the variation of time θ are crucial and will be described in detail in the following subsections.

B. Effects of the timing θ and natural growth rate r

Next, we will focus on the way in which the timing of insecticide application affects moth density [32]. When θ=1, our system is basically the same as that in [15], and we can conclude that when the insecticide efficiency is higher, the

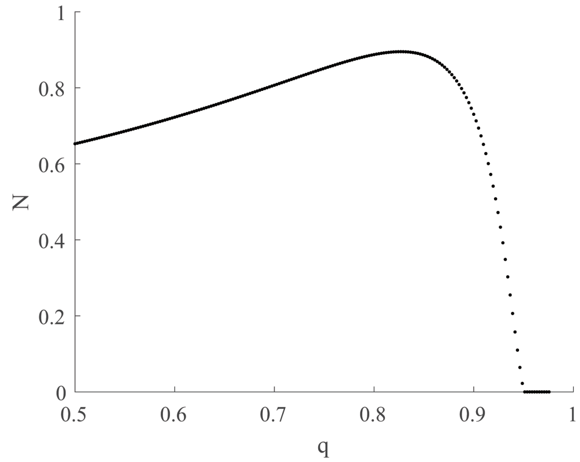

(a) $\theta = 0.1$

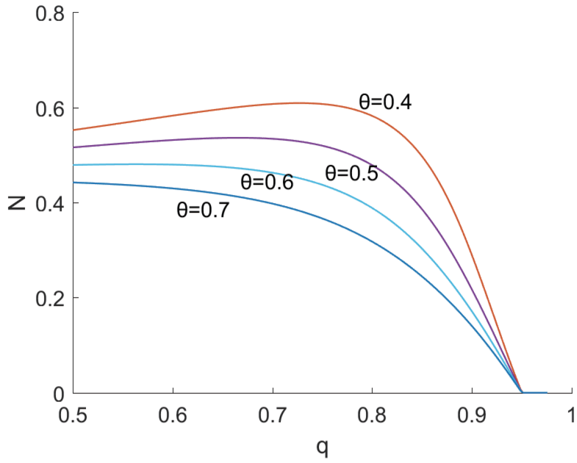

(b) Different values of θ

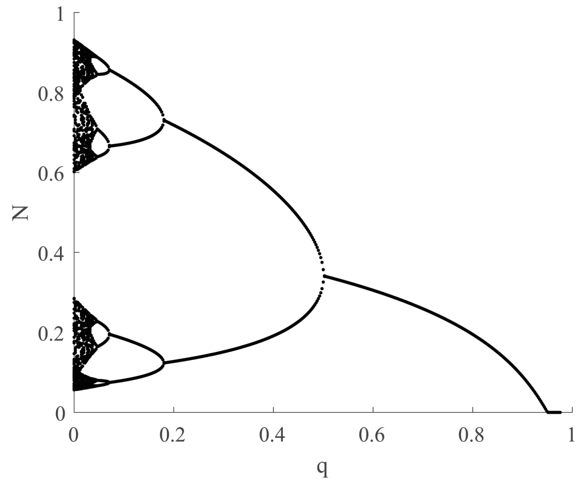

(c) $\theta = 1$

Fig. 4: Effect of different θ on moth population density. The parameter $r = 3$, and the other parameter values are listed in Fig. 3 .

moth density is lower. If the insecticide is placed at each seasonal observation point, there is no contradictory effect; hence, increasing the insecticide efficiency is beneficial for controlling the moth density. Thus, in this case, to control the moth density, we need to improve the efficiency of insecticides. However, in reality, our seasonal observation points often do not coincide with the timing of insecticide placement. Further, the seasonal observation points also have some uncertainty and randomness; hence, we must focus more on $\theta < 1$.

In Fig. 4, we plot the change in population size for different values of θ. We can see that when θ is reduced and falls below a given level, the rising mortality from insecticides leads to an increase in larch budmoth density; hence, the hormetic effects occur. As seen in Fig. 4(b), for intermediate values of θ, the greater the θ, the greater is the relative decrease in larch budmoth density; however, as shown in Fig. 4(c), depositing insecticides at observation sites is not the best option for suppressing moth growth. Hence, choosing the right timing to drop the insecticides is crucial.

In Fig. 5, we plot the effect of the timing of insecticide delivery and the mortality rate of the insecticide (θ, q) on larch budmoth density at different r. From Fig. 5, we can see that the stability without the paradox region of the positive fixed point shrinks sharply as r increases, and the chaotic region expands sharply, with the region showing significant differences. Moreover, we also find that the population size is poorly controlled if the mortality rate of the insecticide is low. The smaller the theta, the more likely is the paradox to occur, again confirming the previous conclusion.

Next, we select two sets of θ values for each r value in Fig. 5 and plot the bifurcation of the moth population as it varies with q, as shown in Fig. 6. For example, in Fig. 6 (a), at $\theta = 0.2$, the population is in an unstable state when $q \in (0, 0.2076)$; the population is in a stable state but there is a paradox when $q \in [0.2076, 0.6832]$; the population is in a stable state but no paradox arises when $q \in (0.6832, 1)$; and $q = 0.6832$ is a paradox inflection point. At $\theta = 0.8$, the population is in an unstable state when $q \in (0, 0.2051)$; the population is in a stable state but no paradox arises when $q \in [0.2051, 1)$, which clearly corresponds to Fig. 5 (a). The same is true for Fig. 6 (b), (c), and (d). We can also see that as r increases, the threshold q that can stabilize the population becomes larger. The area of chaos increases in Fig. 6; this makes it more difficult for us to control the population. Hence

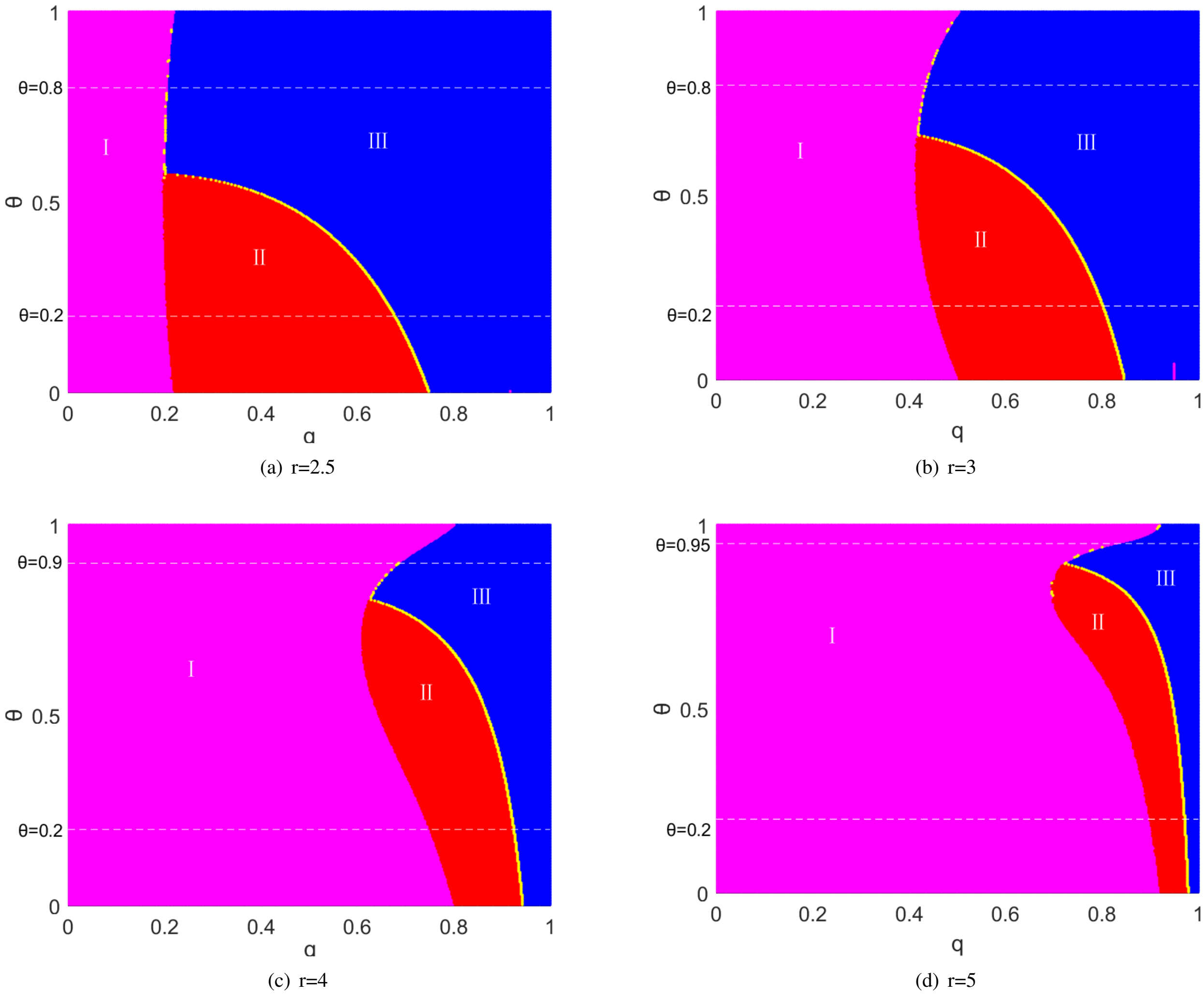

(a) r=2.5

(b) r=3

(c) r=4

(d) r=5

Fig. 5: Effect of insecticide timing and insecticide mortality (θ, q) on moth density N_n at different values of r; the other parameter values are the same as those in Fig. 3. (Chaotic regions are shown in purple (area I); positive fixed point stability without paradox is shown in blue (area III); positive fixed point stability with paradox in red (area II); paradoxical inflection points).

this suggests that the larch budmoth 's natural growth rate is strongly linked to the creation of paradox effects. Therefore, based on the population kinetics, the rational selection of timing of insecticide delivery as well as the mortality rate of the insecticide play an important role in suppressing larch budmoth growth.

C. *Cumulative effects of pesticides*

The analysis presented above shows that we can control pest growth by performing multiple insecticide applications in a season if the first insecticide application is unsuccessful. Depending on the frequency of moth density outbreaks and the limited larch resources, we adopt the chemical control strategy of multiple insecticide injections in each moth generation. For this purpose, we suppose that the pesticide is sprayed m times in a generation $[n, n+1]$, which satisfies $n \le n+\theta_1 < n+\theta_2 < \cdots < n+\theta_m \le n+1$. System (1) can be transformed into the following equation according to [33] at each time point $n+\theta_i$.

$$\begin{cases} N_{t+1} = \prod_{i=1}^{m} p_i N_t \left[\sum_{i=0}^{m} \left(\Delta\theta e^{r\left(Q_t - \frac{\prod_{j=0}^{i} p_j N_t}{k}\right)} \right) \right] \\ Q_{t+1} = (1-b) + bQ_t - \left[\sum_{i=0}^{m} \left(\Delta\theta \frac{\prod_{j=0}^{i} p_j c N_t}{d + \prod_{j=0}^{i} p_j N_t} \right) \right] \end{cases} \tag{26}$$

where $\Delta\theta_i = \theta_{i+1} - \theta_i$, $i = 0, 1, 2, 3...m$. To avoid loss of generality, we assume that $\theta_0 = 0, \theta_{m+1} = 1 \quad and \quad p_0 = 1$.

First, we choose the number of insecticide doses $m = 2$. In Fig. 7, we graphically show how the timing of insecticide delivery and insecticide mortality affect stable population size N^*. Clearly, the timing of insecticide delivery has a significant effect on N^*; the later the insecticide is delivered, the more effectively will the larch budmoth population be reduced. Thus, the paradox can be avoided. In addition, the mortality rate of insecticides applied at different times has the effect of stabilising larch budmoth populations N^*.

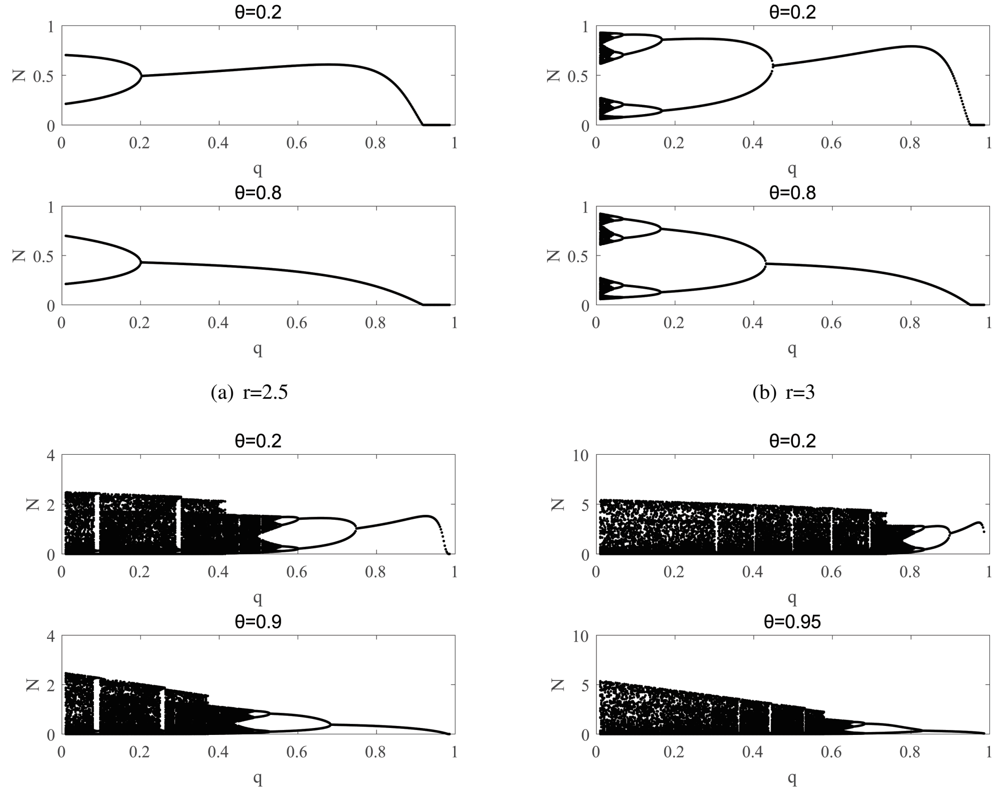

(a) r=2.5

(b) r=3

(c) r=4

(d) r=5

Fig. 6: Bifurcation diagram at a particular value of θ selected from Fig. 5. The other parameter values are the same as those in Fig. 3.

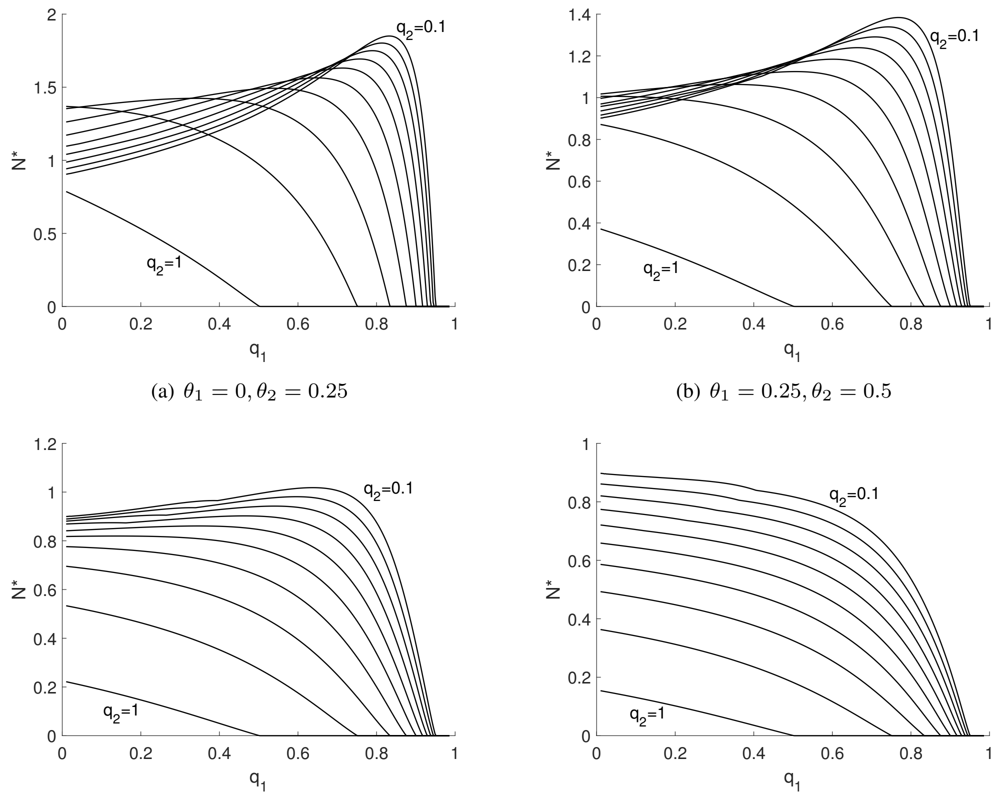

(a) $\theta_1 = 0, \theta_2 = 0.25$

(b) $\theta_1 = 0.25, \theta_2 = 0.5$

(c) $\theta_1 = 0.5, \theta_2 = 0.75$

(d) $\theta_1 = 0.75, \theta_2 = 1$

Fig. 7: Effect of q_1 on the population size of system (26) for different q_2 at different θ_1 and θ_2. The parameters $c = 0.1$; $d = 0.1$; $b = 0.2$; $k = 1$; $r = 3$.

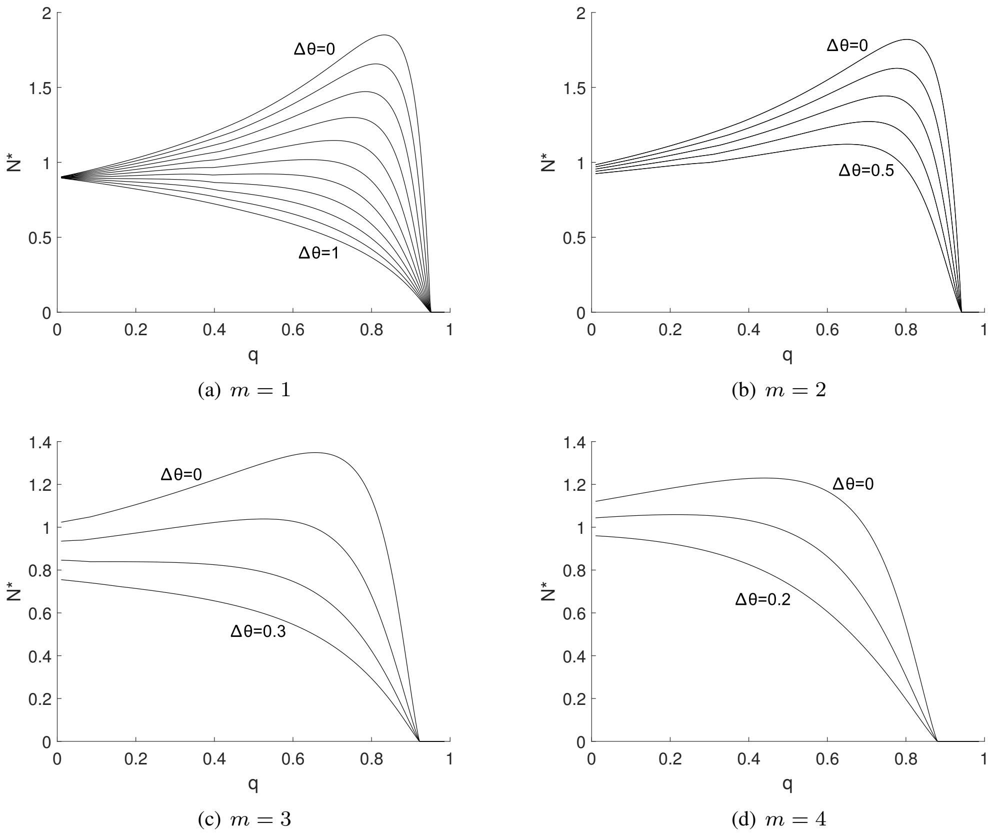

(a) $m = 1$ (b) $m = 2$

(c) $m = 3$ (d) $m = 4$

Fig. 8: Effect of different $\Delta\theta$ on the moth population size of system (26) with varying q. The other parameter values are the same as those in Fig. 7, and $m = 1, 2, 3, 4$ in (a), (b), (c), (d), respectively.

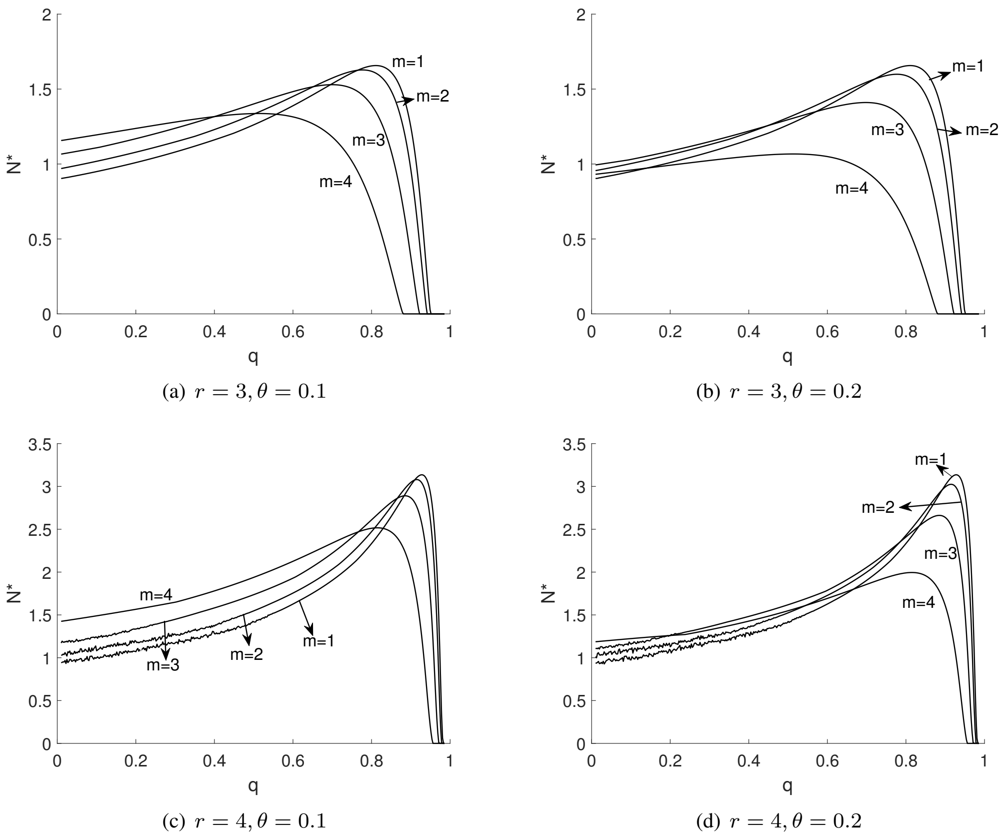

(a) $r = 3, \theta = 0.1$ (b) $r = 3, \theta = 0.2$

(c) $r = 4, \theta = 0.1$ (d) $r = 4, \theta = 0.2$

Fig. 9: Effect of different cumulative numbers of insecticide applications on moth populations in system (26). The other parameter values are the same as those in Fig. 7, and $r = 3$ in (a), (b), $r = 3$ in (c), (d).

More precisely, when the mortality level q_1 is higher, adding q_2 leads to the suppression of the larch budmoth growth; however, if q_1 is small, raising q_2 will instead result in an outbreak of larch budmoth.

In Figs. 8 and 9, we plot the effect of the number of insecticide applications on N^*. For convenience, we take $m = 1, 2, 3, 4$, where $\theta_0 = 0$, $\theta_m + 1 = 1$, $\theta_{i+1} = \theta_i + \Delta\theta$ $(i = 0, 1, 2..., m)$. From Fig. 8, we can see that regardless of how many insecticide applications are made in a season, they do not inhibit population growth, if both the mortality rates q and the time interval $\Delta\theta$ are relatively small. This further confirms that the cumulative effect of incorrect pesticide use can lead to more serious pest outbreaks. Moreover, as shown in Fig. 8, increasing $\Delta\theta$ can effectively reduce the population size for the same number of insecticide applications. In addition, the value of the threshold q_c decreases with the cumulative number of times rises. In Fig. 9, we can see that both threshold q_c and N^* under threshold q_c reduce with the cumulative number of time rises and $\Delta\theta$ increases. However, multi-killing can instead increase the number of pests when the mortality rate is low. In addition, as we are drawing $\overline{N^*}$, the figure oscillates, i.e., it is in a chaotic state. As shown in Figs. 9 (c) and (d), a smaller number of applications at increasing r values can have a chaotic effect and be detrimental to the control of moth populations. Consequently, the cumulative number of pesticide applications, timing of insecticide spraying, and insecticide mortality rates are all critical for the control of larch budmoth populations.

VI. Conclusion

We extended the model in [15] to include chemical controls to describe the inhibitory effect of insecticides on budmoth as well as to consider the effect of insecticides at any time within the two observation sites. On this basis, a discrete time model between plant quality and larch budmoth was proposed, and the effects of the timing and efficiency of the insecticides on the growth of the budmoth were further analyzed. It should be noted that existing studies [15], [16] have only discussed the general dynamic behaviors, and they did not study the complex relationship generated after the addition of chemical control. Through this study, the paradoxical phenomenon of the model was mitigated.

Initially, we proved and numerically simulated the existence of positive fixed points, and analyzed the parameter conditions required for local asymptotic stability of unique positive fixed points according to the Jury condition. Then, the period-doubling bifurcation and Neimark-Sacker bifurcation existence conditions were analyzed using the central manifold theorem and bifurcation theory. Next, numerical simulation was carried out. We found that for certain values of the natural growth rate r and insecticidal timing θ, pesticides with low efficiency will stimulate the growth of the budmoth, and high strength of pesticides can inhibit the growth of the moth. The paradoxical effect is produced, as shown in Fig. 3- Fig. 6. In practice, farmers will choose to kill insects multiple times in a season when one time is not effective. Therefore, we also studied the cumulative effect of insecticides, and the results showed that when the number of insecticides was constant and the insecticide was applied late, the paradox did not easily occur, and the insecticide effect was better, in addition, it is also closely related to the concentration of pesticides twice. As shown in Fig.7-Fig.9, increasing the time interval between two insecticide sprays was also effective in reducing moth populations. And increasing the number of killing insects in a season can reduce the q_c of the paradox inflection point, which is a pest control measure.

In summary, a new model was proposed to study its complex dynamic behavior. Note that this study showed that the natural growth rate of budmoth, the efficiency of insecticides, and the timing of insecticide spraying have a strong impact on the growth of budmoth. Therefore, in the process of agricultural control, the timing and intensity of pesticide spraying should be carefully considered in the implementation of chemical control strategies. In addition, multiple killing strategies should be carried out according to the growth of pests to avoid paradoxical behaviors in the process of pest control.

References

[1] M. He, S. Tang, R. A. Cheke, A holling type ii discrete switching host-parasitoid system with a nonlinear threshold policy for integrated pest management, Discrete Dynamics in Nature and Society 2020 (2020).

[2] R. L. Metcalf, W. H. Luckmann, Introduction to insect pest management, John Wiley Sons, (1975).

[3] S. Tang, Y. Xiao, R. A. Cheke, Multiple attractors of host-parasitoid models with integrated pest management strategies: eradication, persistence and outbreak, Theoretical Population Biology 73 (2) (2008) 181–197.

[4] H. J. Beckie, R. Busi, F. J. Lopez-Ruiz, P. A. Umina, Herbicide resistance management strategies: how do they compare with those for insecticides, fungicides and antibiotics?, Pest Management Science (2021).

[5] S. D. Lane, N. J. Mills, W. M. Getz, The effects of parasitoid fecundity and host taxon on the biological control of insect pests: the relationship between theory and data, Ecological Entomology 24 (2) (2010) 181–190.

[6] C. Iltis, J. Moreau, P. Hübner, D. Thiéry, P. Loupre, Warming increases tolerance of an insect pest to fungicide exposure through temperature-mediated hormesis, Journal of Pest Science (2021) 1–13.

[7] Din, Qamar, Global behavior of a plant-herbivore model, Advances in Difference Equations 2015 (1) (2015) 2015:119.

[8] Q. Din, T. Donchev, Global character of a host-parasite model, Chaos Solitons Fractals 54 (2013) 1–7.

[9] Q. Chen, Z. Teng, Z. Hu, Bifurcation and control for a discrete-time prey-predator model with holling-iv functional response, International Journal of Applied Mathematics and Computer Science 23 (2) (2013) 247–261.

[10] T. Matsuoka, H. Seno, Ecological balance in the native population dynamics may cause the paradox of pest control with harvesting, Journal of Theoretical Biology 252 (1) (2008) 87–97.

[11] J. G. Morse, Agricultural implications of pesticide-induced hormesis of insects and mites, Human Experimental Toxicology 17 (5) (1998) 266.

[12] J. H. Perkins, The shift from ddt. (book reviews: Insects, experts, and the insecticide crisis), Science 217 (1982) 821–822.

[13] R. Guedes, G. C. Cutler, Insecticide-induced hormesis and arthropod pest management, Pest Management Science 70 (5) (2014) 690–697.

[14] S. Tang, J. Liang, C. Xiang, Y. Xiao, X. Wang, J. Wu, G. Li, R. A. Cheke, A general model of hormesis in biological systems and its application to pest management, Journal of the Royal Society Interface 16 (157) (2019).

[15] I. Ali, U. Saeed, Q. Din, Bifurcation analysis and chaos control in a discrete-time plant quality and larch budmoth interaction model with ricker equation, Mathematical Methods in the Applied Sciences (2019).

[16] R. J. Jang, J. L. Yu, Models of plant quality and larch budmoth interaction, Nonlinear Analysis 71 (12) (2009) e1904–e1908.

[17] H. Zhang, Dynamics of larch budmoth-plant quality interaction modelt2, Journal of Heilongjiang Institute of Science and Technology (2007).

[18] S. Ahmad, On the nonautonomous volterra-lotka competition equations, Proc. Amer. Math. Soc. (1993).

[19] Z. Zhan, Stable periodic solutions in a discrete periodic logistic equation, Applied Mathematics Letters 16 (2) (2003) 165–171.

[20] X. Liu, A note on the existence of periodic solutions in discrete predator–prey models, Applied Mathematical Modelling 34 (9) (2010) 2477–2483.
[21] Z. Hu, Z. Teng, Z. Long, Stability and bifurcation analysis of a discrete predator–prey model with nonmonotonic functional response, Nonlinear Analysis Real World Applications 12 (4) (2011) 2356–2377.
[22] Z. Ming, C. Li, J. Wang, Z. Feng, Bifurcation analysis of the three-dimensional hénon map, Discrete and Continuous Dynamical Systems - Series S 10 (3) (2017) 625–645.
[23] S. Tang, G. Tang, R. A. Cheke, Optimum timing for integrated pest management: Modelling rates of pesticide application and natural enemy releases, Journal of Theoretical Biology 264 (2) (2010) 623–638.
[24] H. Seno, A paradox in discrete single species population dynamics with harvesting/thinning, Mathematical Biosciences 214 (1-2) (2008) 63–69.
[25] M. Zhao, C. Li, J. Wang, Complex dynamic behaviors of a discrete-time predator-prey system, Journal of Applied Analysis Computation 7 (2) (2017) 478–500.
[26] Z. He, L. Xin, Bifurcation and chaotic behavior of a discrete-time predator–prey system, Nonlinear Analysis Real World Applications 12 (1) (2011) 403–417.
[27] Z. Jing, J. Yang, Bifurcation and chaos in discrete-time predator-prey system, Chaos Solitons Fractals 27 (1) (2006) 259–277.
[28] E. A. Grove, G. Ladas, Periodicities in nonlinear difference equations, Chapman Hall/CRC, (2002).
[29] A. E. Owoyemi, I. M. Sulaiman, M. Mamat, S. E. Olowo, Stability and bifurcation analysis in a fractional-order epidemic model with sub-optimal immunity, nonlinear incidence and saturated recovery rate, International Journal of Applied Mathematics 51.0 (2021).
[30] Y. A. Kuznetsov, Elements of applied bifurcation theory, applied mathematical sciences 288 (2) (2004) 715–730.
[31] J. Guckenheimer, P. Holmes, Nonlinear oscillations, dynamical systems, and bifurcations of vector fields, Physics Today 38 (11) (1993) 102–105.
[32] Q. Li, Y. Xiao, Bifurcation analyses and hormetic effects of a discrete-time tumor model, Applied Mathematics and Computation 363 (2019) 124618.
[33] X. Wang, Z. Xu, S. Tang, R. A. Cheke, Cumulative effects of incorrect use of pesticides can lead to catastrophic outbreaks of pests, Chaos Solitons Fractals 100 (2017) 7–19.